LM-02K136
January 3, 2003

Improved Thermophotovoltaic (TPV) Performance Using Dielectric Photon Concentrations (DPC)

P.F. Baldasaro, P.M. Fourspring

NOTICE

02K.36

IMPROVED THERMOPHOTOVOLTAIC (TPV) PERFORMANCE USING DIELECTRIC PHOTON CONCENTRATIONS (DPC)

P F Baldasaro, P M Fourspring

Lockheed Martin Company,
Schenectady N.Y.

ABSTRACT

This report presents theoretical and experimental results, which demonstrate the feasibility of a new class of thermophotovoltaic (TPV) energy converters with greatly improved power density and efficiency. Performance improvements are based on the utilization of the enhanced photon concentrations within high refractive index materials. Analysis demonstrates that the maximum achievable photon flux for TPV applications is limited by the lowest index in the photonic cavity, and scales as the minimum refraction index squared, n^2. Utilization of the increased photon levels within high index materials greatly expands the design space limits of TPV systems, including: a 10x increase in power density, a 50% fractional increase in conversion efficiency, or alternatively reduced radiator temperature requirements to as low as ~1000°F.

I. INTRODUCTION AND SUMMARY

Current TPV systems are configured as shown in Figure 1, and include: 1) a thermal photon radiator, 2) a thermal insulating vacuum gap to inhibit parasitic heat conduction, 3) a front surface filter to provide photon spectral control so that parasitic photon absorption ($E<E_g$) is minimized, and 4) a diode with bandgap E_g to convert the usable photonic energy ($E >E_g$) into electric power. *The thermal insulating vacuum gap in existing* TPV systems is ~20 mils thick, much larger than the wavelength of above-bandgap photons of ~1 - 2 microns. The use of a "large" insulating gap as in existing TPV systems will be referred to as "far field" TPV in subsequent discussions.

The analyses below show that the dimension and composition of the insulating gap significantly affect achievable photon flux levels and overall TPV performance. It will be shown that photon flux is in theory only limited by the lowest index of refraction (n) in the transport path between the radiating surface and the active region of diode, and is theoretically as much as n^2 $(\sim 3.5)^2$ times that of the far field case. Recent work completed by Draper Lab *(Reference 1), and Lockheed Martin Company has demonstrated* the feasibility of novel configurations with which to enhance TPV power density and efficiency performance by utilization of the increased photon concentrations available within high refractive index media. The discussion below presents theoretical and experimental results which demonstrate the feasibility of enhanced photon fluxes utilizing the concept of Dielectric Photon Concentration (DPC), and describes the expanded TPV design space.

II. DISCUSSION

Analytical Basis

The following analysis provides a thermodynamic basis for the viability of increased photon transfer using high index materials, referred to in subsequent discussion as Dielectric Photon Concentration (DPC). Analysis begins with reference to the classical derivation of thermal radiation emission found in the literature (Reference 2), based on the notion of a blackbody cavity as in Figure 2, in which there exist a number of allowable photon modes in free space. The number of wave modes in one dimension is equal to the cavity dimension L divided by the free space wavelength λ_s, and the three dimensional mode density is $(L/\lambda_s)^3$. Reference 3 defines the blackbody cavity, free space volumetric energy density integrated over all wavelengths as $U_s = 4\sigma T^4/c$, where σ is the Stefan-Boltzman constant, T is the cavity temperature, and c is the speed of light in vacuum.

A generalized Plankian approach considers a cavity of arbitrary refractive index n_d and presents a view of travelling photons within an index n medium, having reduced wavelength $\lambda_d = \lambda_s/n_d$. The reduced wavelength within the dielectric leads to an increased volumetric wave density ($1/\lambda_d^3 = n_d^3\ 1/\lambda_s^3$), and a corresponding n_d^3 increase in volumetric energy density over that of free space to $n_d^3\ U_s$. In essence, the dielectric medium has more waves, and therefore more energy. It is possible to utilize the full $n_d^3\ U_s$ photon energy density within dielectric media for TPV energy conversion, with proper understanding of cavity photonics, as discussed below.

Cavity Photonics

The analysis below demonstrates that photon transport within dielectric media is controlled by thermodynamic considerations. Consider the equilibrium photonic system in Figure 3a, having a black radiator (absorbtivity A=1) in contact with a zero absorption dielectric medium (transmissivity T=1) and a perfect reflector (reflectivity R=1). In equilibrium (no temperature gradient), the photon flux is isotropic, with no preferred direction in space. This situation changes with the introduction of a temperature gradient such as a "cooled" low temperature absorbing diode (A=1) as in Figure 3b. In this case, the photon flux from the high temperature side (radiator) is higher than from the low temperature side, causing a net photon flux from the hot radiator to the cold diode.

The steady state photon flux in the non-equilibrium Figure 3b system can be calculated in terms of a perturbation to the "equilibrium" photon angular dispersion, assuming that the dielectric photonic energy density ($n_d^3\ U_s$) remains constant in the steady state. This approximation is referred to in the literature as the pseudo-equilibrium approximation. The energy flux E across the dielectric/diode interface in Figure 3b (from n_d to n_{TPV}) can be calculated as the product of the dielectric internal energy density $n_d^3 U_s$ times the angle weighted velocity c_{eff} across the dielectric/diode interface:

$$c_{eff} = \int \frac{c}{n_d} \cos\theta \frac{d\Omega}{4\pi} = \frac{1}{2} \int_0^{\theta_{crit}} \frac{c}{n_d} \sin\theta \cos\theta d\theta = \frac{c}{4n_d} \sin^2(\theta_{crit}) \qquad EQ(1)$$

where $\cos\theta$ represents the photon velocity component normal to the interface, and Ω is the solid angle ($d\Omega = 2\pi \sin\theta d\theta$). θ_{crit} is given by Snell's Law :

For $n_d > n_{TPV}$, $\theta_{crit} = \sin^{-1} (n_{TPV}/n_d)$ EQ(2a)

For $n_d < n_{TPV}$, $\theta_{crit} = \pi/2$ EQ(2b)

Substituting EQ(2a) and EQ(2b) into EQ(1) gives:

$$\textit{For} \quad n_d > n_{TPV} \quad c_{eff} = \frac{c}{4} \frac{(n_{TPV})^2}{(n_d)^3} \quad \textit{and} \quad E = c_{eff} n_d^3 U_{FS} = n_{TPV}^2 \frac{c}{4} U_{FS} \qquad EQ(3a)$$

$$\textit{For} \quad n_d < n_{TPV} \quad c_{eff} = \frac{c}{4n_d} \quad \textit{and} \quad E = c_{eff} n_d^3 U_{FS} = n_d^2 \frac{c}{4} U_{FS} \qquad EQ(3b)$$

EQ(3a) and EQ(3b) show that photon flux from the dielectric medium to the diode proceeds with an asymmetric angle-averaged velocity that is determined by the interface indices, and that the net flux is determined by the "lowest" system index. The EQ(3) result leads to a fundamental conclusion with respect to potential TPV performance:

"TPV system photon flux is limited by the lowest refraction index in the transport path"

The above result is basically a statement of energy conservation, recognizing that photon energy density is determined by the material dielectric index n, and that the lowest photon density medium therefore controls the net photon flux. This result generalizes to any series of dielectric media, and it may be concluded that photonic energy transfer is limited by the lowest energy density (lowest index) medium in a series. In far field TPV, the maximum photon flux is determined by the index of free space, i.e., 1, and represents a lower limit of performance.

TPV Configuration Options

The key engineering challenge in harnessing the potential gains with DPC is to eliminate the low index vacuum gap currently employed in far field TPV systems, while still minimizing parasitic heat conduction between the radiator and diode. Two possible DPC configurations for TPV application are shown in Figure 4: 4a) use of sub-micron radiator/dielectric close-spacing, or 4b) use of a thermally insulating dielectric.

a. Close-Spaced Concept

One approach to maintain radiator/diode thermal insulation is to employ a sub-micron vacuum gap between the radiator and the diode, as proposed by Draper Lab and shown in Figure 4a. In this concept, photons essentially "tunnel" across the sub-micron gap, while parasitic phonon energy having a much smaller characteristic wavelength is isolated from transport. The tunneling process is described and formulated in the appendix. The advantages of the close-spaced approach are the possible "controllability" of the gap for active photon flux control, and the possibility for a low temperature spectral control device. The disadvantages are the need for a controllable sub-micron gap, and a vacuum system to minimize parasitic energy transfer.

b. Dielectric Insulator Concept

A second approach to maintain radiator/diode thermal insulation is shown in Figure 4b, and involves the use of an insulating dielectric medium in direct contact with both the radiator and diode. In this concept, the insulator serves double purpose as both thermal insulator and high refraction index medium. The advantage of this concept is the elimination of the need for a vacuum gap, and the disadvantages are thermal stress concerns in the dielectric media, and the potential for increased parasitic photon absorption in the high index dielectric insulator.

Experimental Results

a. Draper Results

The Draper experimental setup is shown in Figure 5a, and models the DPC concept in Figure 4a. A 400°C silicon radiator is moved from > 4 microns (far field) to ~0.2 microns from a 0.6 eV InGaAs TPV diode. The radiator / diode spacing of ~0.2 microns is determined by prefabricated spacer structures. The data shown in Figure 5b demonstrate an increase in short circuit current over the far field case of ~6x, consistent with analysis. The absolute value of the measured short circuit currents are consistent with the radiator temperature and diode bandgap, and represents about half the theoretical value of $n^2 \sim 3.4^2$ or 12. The measured open circuit voltage scales with the diode equation, i.e., a 6x increase in current increases voltage by kTln6 (~42 mV).

b. Lockheed Martin Company Results

The Lockheed Martin Company experimental setup is shown in Figure 6, and is intended to model the DPC concept 4b. This experiment employs a 590 nm light emitting diode (LED) as the "heat" source, coupled to a ~1.1 eV silicon diode (solar cell). An index matched dielectric fluid (n=1.5) couples the light source directly to the diode. Photon enhancement is quantified by the photon flux increase observed when the dielectric oil is inserted between the LED and the diode. The measured enhancement (see Table 1) of 1.90x in photon flux is consistent with predictions using a coupling dielectric fluid with an $n^2 \sim 2.25$.

III DPC APPLICATIONS

III.1 Potential TPV Performance Gains

Power Density

The most straightforward gain with DPC is increased power density as calculated in Figure 7 versus refractive index. Existing III-V diode systems being evaluated for TPV application have refraction indices of ~3.5, which places a limit of ~12x on the photon flux enhancement relative to existing far field TPV systems. This gain is independent of increased power density from increased conversion efficiency, as discussed below.

Efficiency

Diode efficiency, η, may be defined as the product of the following fundamental parameters:

$$\eta = F_o V_{oc}/E_g \; ff \; QE \qquad EQ(4)$$

where:
- F_o = Fraction of usable above-bandgap energy
- V_{oc}= Open circuit voltage
- E_g = Diode bandgap
- ff = Fill factor
- QE = Quantum efficiency

The enhanced photon flux available with dielectric concentration offers potential gains in all four efficiency parameters in EQ(4) as discussed below.

Reference 4 defines V_{oc} and ff in terms of thermodynamic variables limited by the J_{sc}/J_r ratio, where: J_{sc} is the short circuit current, and J_r is the dark current coefficient. The increased photon flux and current levels available with DPC can increase diode voltage, as indicated by the diode equation:

$$V_{oc} = k_B T_c \ln(J_{sc}/J_r) \qquad EQ(5)$$

A 12x increase in J_{sc} increases open circuit voltage by ~.07 V for fixed J_r, or roughly a fractional 25% increase above existing far field TPV systems. Similarly, the Reference 4 work indicates a 7% fractional gain in fill factor is theoretically achievable with a 12x increase in J_{sc}. However, potential gains in diode voltage and fill factor are limited, even though EQ(5) would predict unbounded voltage as the refraction index and J_{sc} increase indefinitely. The thermodynamic limit on voltage is explained in Reference 4 and repeated below.

In general, J_r has contributions from several sources including: Shockley-Read Hall (SRH), Auger, and radiative recombination processes. While SRH and Auger processes can in theory be negligible, there is a lower limit on J_r from radiative recombination, resulting from equilibrium blackbody radiation emanating from the diode surface at temperature T_c. The thermodynamic J_r limit can be calculated by integrating the diode Blackbody emission spectrum over the full range of photon frequencies from the bandgap frequency to infinity, and is given from Reference 2 as:

$$J_r \approx n^2 A_1 T_c \exp\left[-E_g / k_B T_c\right] \qquad \text{EQ(6)}$$

where: A_1 is a constant, and n is the dielectric index of the radiator / diode medium.

EQ(6) shows that the thermodynamic limit on reverse current J_r increases as n^2, just as the limiting short circuit current J_{sc}. Therefore DPC has no effect on the thermodynamic limit of J_{sc}/J_r, and therefore diode performance. However, most diode systems are limited by mechanisms other than thermodynamic radiative emission from the diode itself; and an increase in J_{sc} can in theory increase performance.

Quantum efficiency (QE) also improves with DPC as a consequence of the unique angular dispersion. Absorption of above-bandgap photons in current far field TPV systems is inhibited by the low photon dispersion angle within the high index diode (~15 degrees) which limits the effective absorption thickness in active diode layers. The angular dispersion of above-bandgap photons in DPC systems is 180 degrees, which increases the effective angle-integrated absorption length by ~ 40%. Better use is therefore made of above-bandgap photons, and a 7% fractional increase in QE is estimated.

Current far field TPV systems suffer efficiency losses caused by photons having energy significantly above the bandgap. The low power density of far field systems necessitates the absorption of high energy above-bandgap photons in order to make power density requirements. However, the increased photon flux available with DPC would permit selective reflection of very high energy photons ($\lambda < 1.3$ micron), for a potential decrease in overheating, and an increase of ~4% fractional in the overheating factor F_o, at a cost of ~10% in maximum power density.

The maximum cumulative gain from the various diode efficiency factors with DPC is estimated as ~50% fractional over existing far field TPV systems.

III.2 Development Challenges

The potential performance gains with DPC are very large, but so are the technical challenges. It is likely that the increased challenges associated with an order of magnitude increase in heat flux and current density will compromise potential performance gains.

Device Temperature Control

The increased heat flux available with DPC poses a problem for diode temperature control. Diode temperature must be maintained as low as possible to maximize conversion efficiency, and in this sense, DPC power density gains conflict with efficiency goals. A highly efficient heat removal system will be required for dielectric concentrated TPV systems.

Diode Performance

A key diode concern associated with a >10x increase in diode current is the potential for increased Auger recombination in low bandgap diodes (~0.5 ev), which in effect increases J_r, and can significantly lower diode voltage. A more detailed evaluation of diode performance is required, and alternative diode architectures and designs may be necessary.

Spectral Control

Spectral control remains a major DPC technology challenge because the spectral dispersion of photonic energy is the same (or worse) than in far field TPV, i.e. the fraction of usable above-bandgap energy is low. The DPC approach introduces new challenges as well as new opportunities as discussed below.

For the close-spaced DPC concept in Figure 4a low temperature spectral control options are still available, but the use of low-index interference filter components is eliminated because of reduced coupling between the radiator and the high index active diode. In addition, the close-spaced concept enhances long wavelength (below-bandgap) energy preferentially, and further increases the spectral control challenge which will be very dependent on achievable gap spacing at the sub-micron level.

For the dielectric insulator concept described in Figure 4b, it may be necessary to place some form of spectral control on the high temperature source to minimize parasitic below-bandgap photon absorption in the insulating dielectric. High temperature will limit materials and configuration options, and introduce lifetime issues.

The DPC concept offers additional spectral control process options because of the unique photon angular dispersion. Initial analysis indicates the possibility of a simplified spectral control strategy for DPC systems employing a single low-index reflection layer (LIR) on the back surface as shown in Figure 8. This approach is similar to the current back surface reflector strategy, in that above-bandgap photons are absorbed by the diode itself, while below-bandgap photons are reflected by the back surface. However, the LIR concept relies on critical angle reflection between the active diode and the low-index layer. Critical angle reflection is very high in theory, because only photons within the high-index diode critical angle (~15 degrees) can pass from the diode into the LIR. Reflection theoretically approaches the value $1-1/n^2$ (>90%).

Networking

The increased heat flux using dielectric concentration generates higher diode electrical currents and I^2R losses in the TPV electrical network. Increased electrical currents of >10x are another threat to overall system efficiency, and will require diode network redesign. These high currents will necessitate smaller current collection areas, and tandem architectures.

Gap Spacing Sensitivity

A unique challenge with the close-spaced DPC approach is control of the sub-micron gap between the radiator and the dielectric receiver, which affects both power density and efficiency as shown in Figure 9. As gap spacing increases above the design point of ~0.1 microns, the coupling of above-bandgap (shorter wavelength photons) decreases most rapidly, reducing both power density and efficiency because of the lower fraction of above-bandgap energy. Even small fluctuations in gap spacing may lead to difficulties in system network performance. The high gap sensitivity also raises additional concerns for lifetime deposition, i.e. gap spacing changing with life.

IV. DPC Design Space Evaluation

Increased Power Density and Efficiency

Figure 10 shows the comparison of far field and DPC radiation flux as a function of radiator temperature, and demonstrates the range of the power density / operating temperature tradeoff. The most straightforward approach with DPC is to increase TPV generator power density. A 10x increase in power density would lead to a significant reduction in generator size and cost, and gains in efficiency as shown above.

Lower Operating Temperature

An alternative approach with DPC is to reduce operating temperature at a fixed power density. Figure 10 shows that a gain of 12x from DPC (n=3.5), translates into a reduction in operating temperature to as low as ~1000. Lower operating temperature eases the challenge associated with radiator materials lifetime, thermal stress, and recuperator fabrication. However, lower operating temperature also increases the spectral control challenge because the fraction of usable energy decreases with lower radiator temperature.

DPC promises both higher power density and conversion efficiency, and may enable use of more developed higher bandgap systems such as GaSb or lattice-matched InGaAs, having increased fabrication flexibility and greatly reduced cost.

V. Required Development

Successful implementation of DPC would have a major impact on existing TPV system performance parameters. This section discusses some key next steps in a potential DPC evaluation program, based on the limited data and technical assessments that have been performed:

Close-spaced gap control measurements

The close-spaced TPV concept requires the development and control of a sub-micron radiator/diode gap, with a high temperature gradient. The physical process that limits the gap spacing is not yet known.

Dielectric Insulator feasibility measurement

The dielectric insulator concept shown in Figure 4b is new and untested. This concept requires the use of a relatively thick dielectric insulator (several millimeters) to inhibit parasitic heat conduction, while still enabling efficient photon transport. Basic testing is required to confirm concept feasibility as well as to quantify technology development needs, and thermal stress tolerance.

High injection diode performance

The utilization of high current levels in low bandgap diodes is unproven, and high current levels can lead to increased Auger recombination and reduced performance. Testing must be done to determine diode performance feasibility.

Low Index Reflector (LIR) feasibility testing

The DPC concept appears to offer an advantage in spectral control process physics via the use of a single, low index dielectric layer on the TPV diode. This concept has been analytically confirmed but not tested experimentally. Spectral control is critical to viable DPC implementation; and the low fraction of usable above bandgap energy makes efficient spectral control difficult to achieve. Experimental design and execution to confirm feasibility of the LIR concept is a key step in proceeding with either the dielectric insulator or close-spaced concept.

Summary

The successful development of DPC has the potential to greatly expand TPV design space. Initial data supports the conceptual feasibility, but many engineering issues remain which could prevent concept practicality. Successful DPC development would alter all of the basic TPV system components, i.e. radiator, diode, and filter technologies.

REFERENCES

1 Enhanced photogeneration of carriers in a semiconductor via coupling across a nonisothermal nanoscale vacuum gap, RS DiMatteo et al, Applied Physics Letters, Vol 79, No. 12, September 17, 2001.

2 Fundamentals of Momentum, Heat, and Mass Transfer, Welty Wicks and Wilson, 1969.

3 Thermal Physics, 2nd edition, C Kittel,1980.

4. Thermodynamic analysis of thermophotovoltaic efficiency and power density tradeoffs, PF Baldasaro et al, J Appl physics, Vol 89, No. 6, March 2001.

TPV Schematic

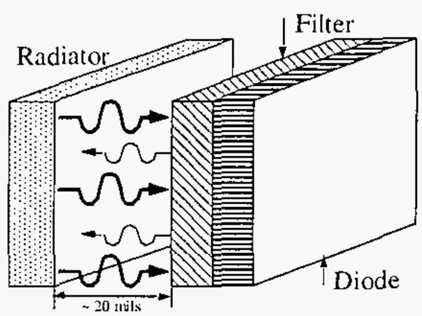

Figure 1

Plankian Wave Modal Density

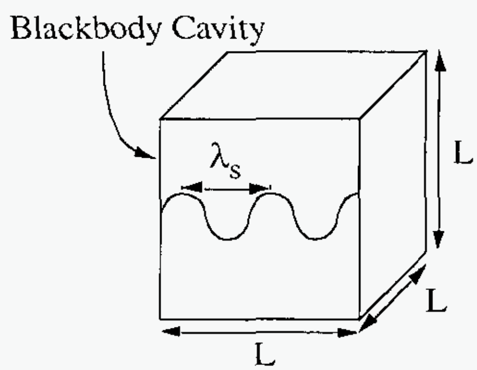

$$N(\lambda) = \left(\frac{L}{\lambda_s}\right)^3$$

$$\frac{N(\lambda)}{Vol} = \frac{1}{\lambda_s^3}$$

Figure 2

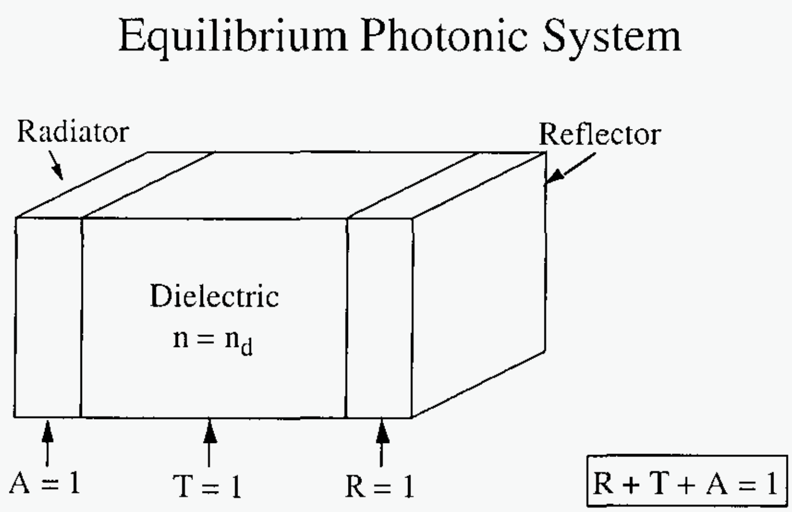

Figure 3a

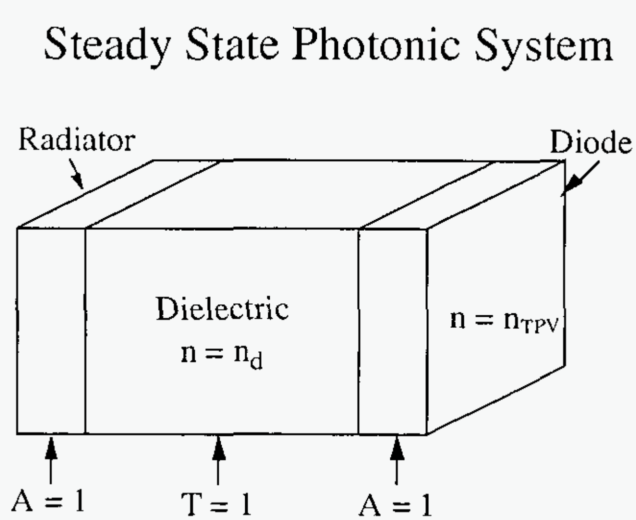

Figure 3b

TPV Close-Spaced Concept

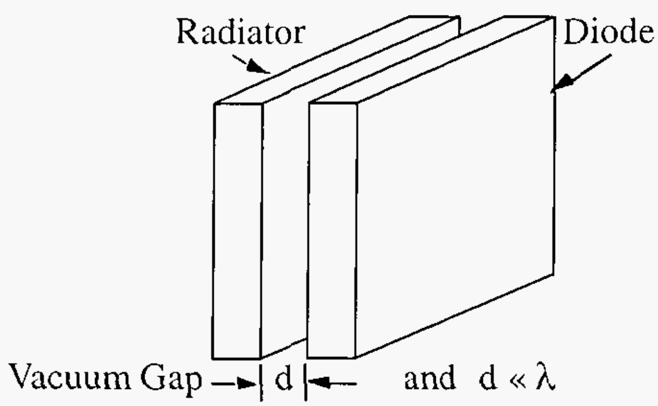

Figure 4a

TPV Dielectric Insulator Concept

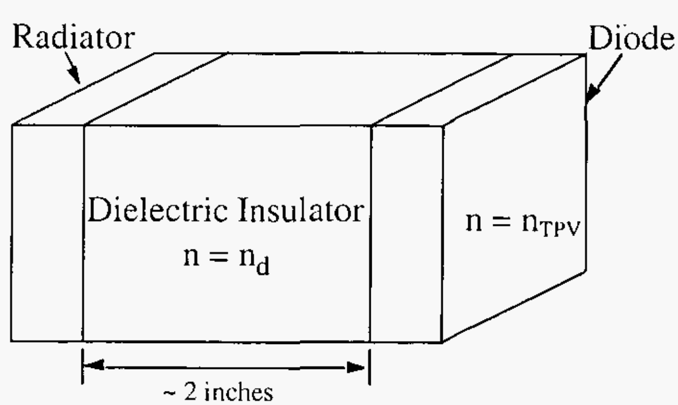

Figure 4b

Draper Lab DPC Experimental Setup

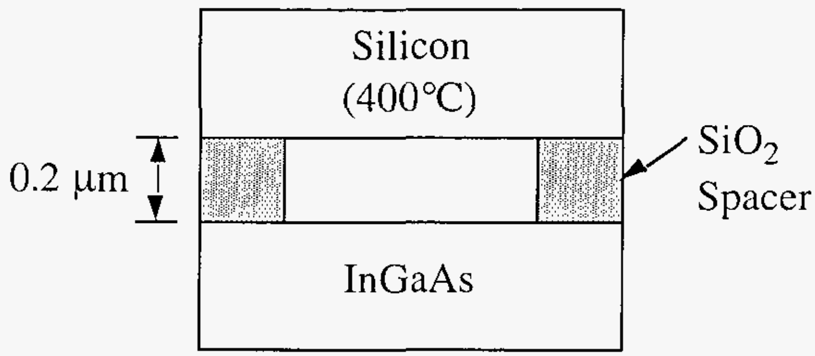

Figure 5a

Unpublished Draper Lab DPC Experimental Results

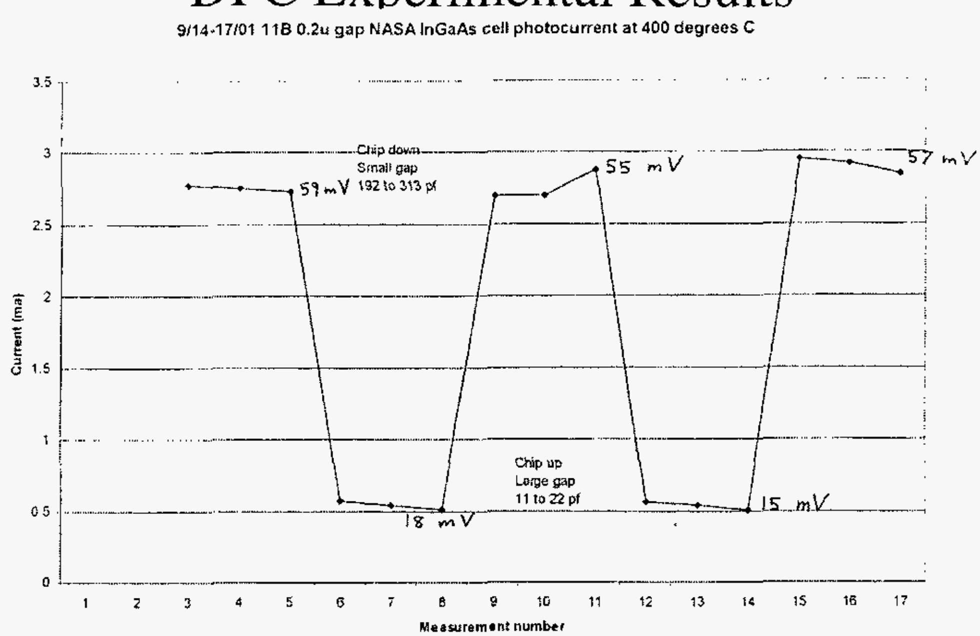

Figure 5b

Lockheed Martin Company DPC Experimental Setup

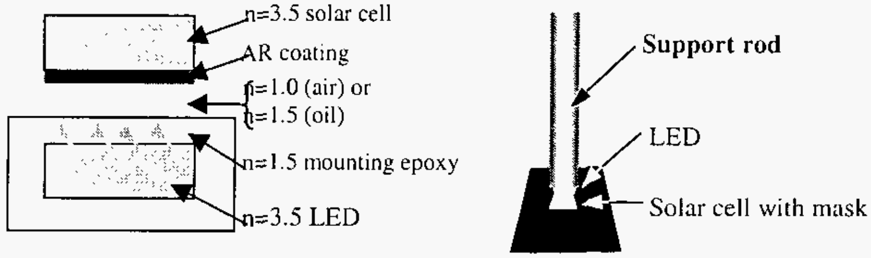

Figure 6

Table 1 Current output from cell with and without an air gap.

Current without oil (μA)	Current with oil (μA)	Factor
267.5	538	2.01
250.1	528	2.11
189.7	359.7	1.90
218.6	404	1.85
250.1	460	1.84
360.3	700	1.94
435	763	1.75
348.5	685	1.97
Average		1.92
Standard Deviation		0.112

TPV Gains with Dielectric Photon Concentration

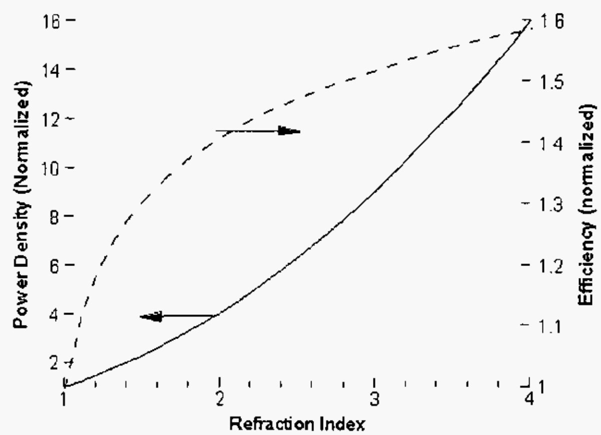

Figure 7

Close-Spaced TPV Low-Index Spectral Control Concept

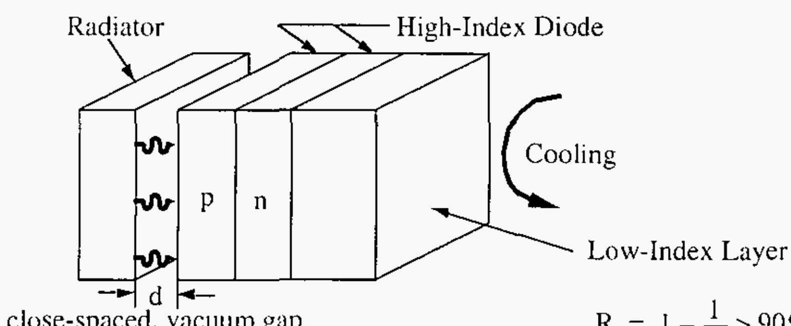

$$R = 1 - \frac{1}{n^2} > 90\%$$

Figure 8

Close-Spaced TPV Gap Sensitivity

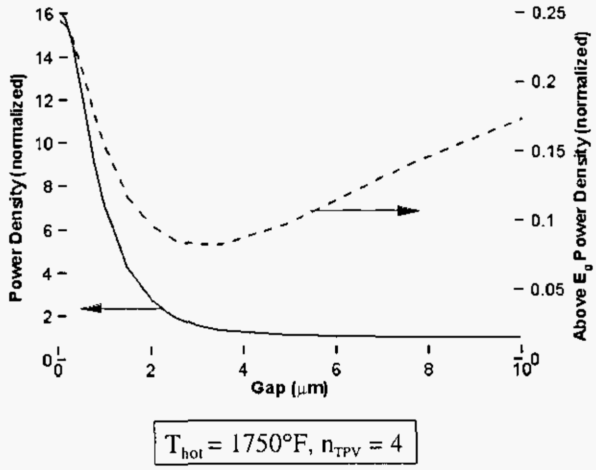

Figure 9

DPC vs. Far Field TPV Power Density

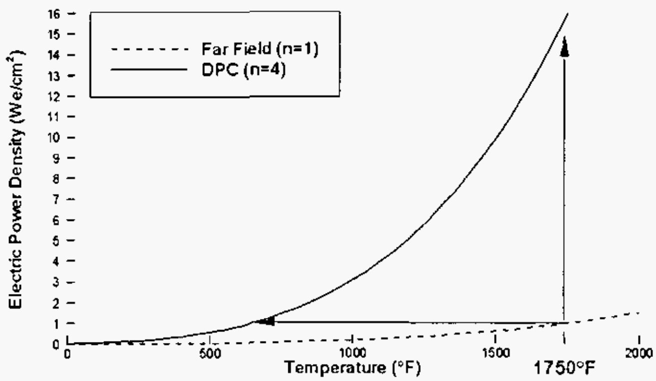

Figure 10

APPENDIX

CLOSE-SPACING TUNNELING ANALYSIS

This appendix presents the analysis of the photon tunneling probability for the application in close-spaced dielectric concentration TPV concept. Figure A-1 describes the physical situation: two dielectric media of index n separated by a gap of thickness d. In the far field instance, where d >> λ, complete photon frustration occurs for photons with angle $\theta > \theta_{crit} = \sin^{-1} 1/n$. However, in the close-spaced case it is necessary to account for finite photon wave penetration into the vacuum gap, and the potential for "photon tunneling".

Analysis begins with consideration of the scalar photon wave equation for zero absorption dielectric media:

$$\nabla^2\phi + n^2\lambda^2\phi = 0$$

Where: ϕ=Electric field strength
n= Refractive index
λ=Photon wavelength

This equation has travelling wave solutions ($e^{ix/\lambda n}$) for real values of n, and decaying solutions ($e^{-x/\lambda}$) in the vacuum gap for angles > θ_{crit}.

Using the notation in Figure A-1, the tunneling probability is calculated as

$$T(\lambda, d, \theta) = (AA^*)/(CC^*)$$

Where A and C are the travelling wave coefficients for the incoming and transmitted waves, and the * symbol denotes complex conjugate. Completion of the algebra leads to the expression:

$$T(\lambda,d,\theta) = 16(n^2(1-\frac{1}{n^2})^2(e^{2\frac{d(\theta)}{\lambda}} - 2 + e^{-2\frac{d(\theta)}{\lambda}}) + 4e^{2\frac{d(\theta)}{\lambda}} + 8 + 4e^{-2\frac{d(\theta)}{\lambda}})^{-1}$$

Where: $d(\theta) = d/\cos\theta$

This expression gives the wavelength, spacing, and angular dependence of photon transport across the close-spaced gap between two equal dielectric media for photon angles $\theta > \theta_{crit}$.

Tunneling Probability Configuration

$n = n_d$ $\qquad$ $n = 1$ $\qquad$ $n = n_d$

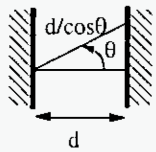

$$\varphi(x) = Ae^{\frac{in_d x}{\lambda}} + Be^{-\frac{in_d x}{\lambda}} \qquad \varphi(x) = Ae^{\frac{in_d x}{\lambda}} + Be^{-\frac{in_d x}{\lambda}}$$

$$\varphi(x) = Fe^{\frac{x}{\lambda}} + Ge^{-\frac{x}{\lambda}}$$

$$\boxed{\nabla^2\varphi + n^2\lambda^2\varphi = 0}$$

Figure A-1